Supporting Information

Lin et al. 10.1073/pnas.1719376115

SI Notes

Derivation of the Observed Rate Constant. For reaction

$$A \underset{k_r}{\overset{k_f}{\rightleftarrows}} B,$$

where k_f and k_r present the rate constants for the forward and reversed reactions, respectively, and [A] and [B] present the concentration of each species in solution,

$$d[A]/dt = -k_f[A] + k_r[B]$$

$$d[B]/dt = k_f[A] - k_r[B]$$

$$_9\text{Since}[B] = [A]_{total} - [A]$$

$$d[A]/dt = -(k_f + k_r)[A] + k_r[A]_{total}.$$

Thus,

$$[A]/[A]_{total} = kr/(kf + kr) + kf/(kf + kr)\exp(-(kf + kr)t)$$

$$\ln([A]/[A]_{total}) = N - k_{obs}t,$$

where k_{obs} is the observed rate constant, t is the reaction time, and

$$N = \ln(k_r/(k_f + k_r)) + \ln(k_f/(k_f + k_r))$$

$$k_{obs} = k_f + k_r.$$

Relation Between the Redox Potential of the Dye and Protein. According to Nernst equation (Eq. S1), the redox potential of the equilibrated solution will relate the concentration ratio of the redox couple $FAD_{ox}/FAD^{\bullet -}$ to that of the dye (Dye_{ox}/Dye_{red}) offset by their standard redox potentials ($E^{o\prime}$; Eq. S2), where R is the gas constant (8.314 $J{\cdot}K^{-1}{\cdot}mol^{-1}$), F is the Faraday constant (96,485 $C{\cdot}mol^{-1}$), T is the absolute temperature, n is the number of electrons transferred during the reaction in moles, and D and P represent the dye and protein, respectively. The relationship between dye and protein potential in millivolts is expressed by Eq. **S4**:

$$E = E^{o\prime} + \frac{RT}{nF}\ln\left(\frac{[Oxidized]}{[Reduced]}\right), \quad \textbf{[S1]}$$

$$E_D^{o\prime} + \frac{RT}{n_D F}\ln\left(\frac{[Dox]}{[Dred]}\right) = E_P^{o\prime} + \frac{RT}{n_P F}\ln\left(\frac{[Pox]}{[Pred]}\right), \quad \textbf{[S2]}$$

$$E_D^{o\prime} + \frac{58}{n_D}\lg\left(\frac{[Dox]}{[Dred]}\right) = E_P^{o\prime} + \frac{58}{n_P}\lg\left(\frac{[Pox]}{[Pred]}\right), \quad \textbf{[S3]}$$

$$\frac{58}{n_D}\lg\left(\frac{[Dox]}{[Dred]}\right) = \frac{58}{n_P}\lg\left(\frac{[Pox]}{[Pred]}\right) + (E_P^{o\prime} - E_D^{o\prime}), \quad \textbf{[S4]}$$

where

$$\frac{[Ox]}{[Red]} = \frac{\Delta A, total}{\Delta A} - 1.$$

SI Materials and Methods

Expression and Purification of dCRY. The plasmid pET-28a containing the dCRY construct was expressed in CmpX13, an engineered *Escherichia coli* cell line containing the riboflavin transporter. As described previously (1), cells were grown in Terrific Broth (IBI) at 37 °C and induced with 0.4 mM isopropyl β-D-1-thiogalactopyranoside and 5 μM FAD after the optical density (OD) at 600 nm reached 0.6–0.8. Cells continued to grow overnight at 17 °C before sonication in lysis buffer containing 50 mM Hepes (pH 8), 400 mM NaCl, 10% glycerol (vol/vol), 0.5 mM Tris(2-carboxyethyl)phosphine (TCEP), and 0.5% Triton X-100 (vol/vol). Cell lysate was centrifuged at 48,000 × *g* for 1 h to remove cell debris. The supernatant was incubated with Nickel-NTA Agarose Beads (Gold Biotechnology) for 45 min and then cleaned with wash buffer containing 50 mM Hepes (pH 8), 400 mM NaCl, 10% glycerol (vol/vol), and 20 mM imidazole. The dCRY was eluted in buffer containing 50 mM Hepes (pH 8), 100 mM NaCl, and 10% glycerol (vol/vol) under an imidazole gradient that varied from 40 to 200 mM. The faint yellow elution solution was further purified by a Superdex 200 size exclusion column in 50 mM Hepes (pH 8), 150 mM NaCl, 10% glycerol (vol/vol), and 2 mM TCEP. Site-directed mutations were made with QuikChange (Agilent), and all DNA was sequenced at the Cornell Biotechnology Center.

UV–Visible Absorption Spectroscopy and Kinetics. UV–visible absorption spectra were measured from 10 μL of dCRY [15 mg/mL; in 50 mM Hepes (pH 8), 150 mM NaCl, 10% glycerol (vol/vol), and 2 mM TCEP] in quartz cuvettes with a pathlength of 2 mm (giving A_{450} = ∼0.35). For the dCRY sample with 2 mM GSH, dCRY is buffer-exchanged into 50 mM Hepes (pH 8), 150 mM NaCl, 10% glycerol (vol/vol), and 2 mM GSH. Spectra were recorded by an Agilent 8453 diode-array spectrophotometer and normalized by setting A_{800} to 0. Kinetics of dCRY photoreduction were monitored at 365 nm, 403 nm, and 450 nm, with a time cycle of 2 s under illumination from a blue laser (TECBL-440, 25 mW, 440 nm; World Star Tech). The light intensity was adjusted by neutral density filters (Thorlabs) and monitored with a power meter. Traces at 450 nm were monitored for ∼15 min until there was no further change. In general, monoexponential functions of the form $A_{450}(t) = A_0e^{-kt} + y_0$ fit the progress curves well, where A_0 is the prefactor, k is the rate constant, and y_0 is the offset caused by background noise and system error.

Steady-State Fluorescence Spectrum. One hundred forty microliters of dCRY sample [4 mg/mL, 50 mM Hepes (pH 8), 150 mM NaCl, 10% glycerol (vol/vol), and 2 mM TCEP] was excited at 450 nm at room temperature, and emission was detected from 460 to 700 nm. Spectra were recorded by an Agilent Cary Eclipse Fluorescence Spectrophotometer.

Native PAGE. Four microliters of dCRY sample [4 mg/mL, 50 mM Hepes (pH 8), 150 mM NaCl, 10% glycerol (vol/vol) and 2 mM TCEP] was covered in the dark or illuminated by blue laser (TECBL-440, 280 W/m^2) for 15 min at room temperature and then mixed with 6 μL of native sample buffer (Bio-Rad), before loading on protein gels (Mini-PROTEAN TGX gel; Bio-Rad). Protein bands are visualized by Coomassie blue staining and quantified by ImageJ (NIH).

Partial Proteolysis. Ten microliters of dCRY [4 mg/mL, 50 mM Hepes (pH 8), 150 mM NaCl, 10% glycerol (vol/vol), and 2 mM TCEP] was digested with 3 μL of trypsin (0.5 mg/mL, T1426,

made fresh; Sigma–Aldrich) at room temperature and then quenched by 3 μL of trypsin inhibitor after 30 s (1 mg/mL; Sigma–Aldrich). The sample was mixed with 5 μL of Laemmli Sample Buffer (Bio-Rad) and heated at 90 °C for 5 min. Five microliters of sample was loaded on a protein gel (Mini-PROTEAN TGX gel) for SDS/PAGE and stained with Coomassie blue. For the light conditions, the dCRY sample was illuminated by blue laser (TECBL-440, 280 W/m^2) for 15 min.

Protein Spectrum Electrochemistry. The dCRY redox potentials were measured by performing a spectrophotometric redox titration with xanthine/xanthine oxidase in the presence of a redox-active dye whose spectral properties report on the solution potential (2). Methyl viologen was used as a redox mediator. The dCRY was buffer-exchanged into 50 mM potassium phosphate buffer (pH 7) and 5% glycerol. One hundred microliters of dCRY (4 mg/mL) with A_{450} = 0.4 was equilibrated with safranin T (A_{498} = ~0.5), 30 μM methyl viologen, and 300 μM xanthine. A mixture of 10 mM glucose, 25 μg/mL glucose oxidase, and 50 μg/mL catalase was prepared new and added 15 min before the titration to create and maintain a low oxygen concentration. The reduction was initiated by 100–200 nM xanthine oxidase. The concentrations of xanthine oxidase and methyl viologen were optimized to ensure simultaneous and slow reduction of the dye and dCRY over the course of about 1 h, without causing interference from reduced methyl viologen in the spectrum. Reduction of WT dCRY by xanthine alone produced an isosbestic point at 498 nm (Fig. S3*B*), thereby confirming that FAD_{ox} is in equilibrium with $FAD^{\bullet-}$ and undergoes no further reduction to a hydroquinone state. FAD absorbance changes at wavelengths of 450 nm and 498 nm were monitored every 10 s. To obtain the absorbance change for complete reduction, 5 mM dithionite was added at the end of the titration. As indicated by Eq. **S5**, log ([oxidized]/[reduced]) of the dye was plotted as a function of log ([oxidized]/[reduced]) for the protein of interest. The intercept then gives the difference in standard redox potential between the protein and dye, whereas the slope reports on the number of electrons transferred:

$$\frac{58}{n_D}\log\left(\frac{[Dox]}{[Dred]}\right)=\frac{58}{n_P}\log\left(\frac{[Pox]}{[Pred]}\right)+\left(E_P^0-E_D^0\right), \qquad \textbf{S5}$$

[where, E^0 is the standard redox potential at pH 7, P represents the protein, D represents the dye, and n represents the number of electrons involved in dye or protein reduction.

To validate this method, we measured the redox potential of another well-studied flavoprotein, the flavin mononucleotide (FMN)-binding domain of nitric oxide synthase (NOS) using Cresyl violet as the reporter dye ($E^{0\prime}$ = −177 mV vs. SHE) (Fig. S3*A*). The measured redox potential of −171 ± 0.5 mV for NOS_{FMN} agrees well with the literature value of −179 mV (3).

Cell Culture Stability Assays. The dCRY, *Drosophila* TIM (TIM, long and short allele), and *Drosophila* JET, or site-directed mutants thereof, were N-terminally tagged with three myc epitopes, C-terminally tagged with three HA epitopes, or C-terminally tagged with a FLAG epitope, respectively, and cloned into the pAc5.1/V5 vector (Invitrogen) using standard cloning protocols. S2 cells were grown in Schneider's medium supplemented with 10% FBS and penicillin/streptomycin. The dCRY was cotransfected with either empty vector or TIM + JET plasmid with Effectene (Qiagen) using the manufacturer's protocols (1:1:2 dCRY/JET/TIM). The cell medium was refreshed after 24 h, and the cells were divided into two populations. Twenty-four hours later, each population was lysed in a modified radioimmunoprecipitation buffer under red light or after being exposed to white light for 1 h (~600 lx or ~5 W/m^2). Equal amounts of lysates were run on 6% SDS/PAGE gels and immunostained using myc (Sigma), HA (Roche), FLAG (Sigma), and tubulin (Sigma) antibodies. Tubulin was used as a loading control. Transfections were performed four times for each variant in dark (red light) and light.

1. Ganguly A, et al. (2016) Changes in active site histidine hydrogen bonding trigger cryptochrome activation. *Proc Natl Acad Sci USA* 113:10073–10078.
2. Massey V (1981) A simple method for the determination of redox potentials. *Flavins and Flavoproteins*, eds Walsh C, et al. (W. DeGruyter & Co., Berlin), pp 59–66.
3. Garnaud PE, Koetsier M, Ost TW, Daff S (2004) Redox properties of the isolated flavin mononucleotide- and flavin adenine dinucleotide-binding domains of neuronal nitric oxide synthase. *Biochemistry* 43:11035–11044.

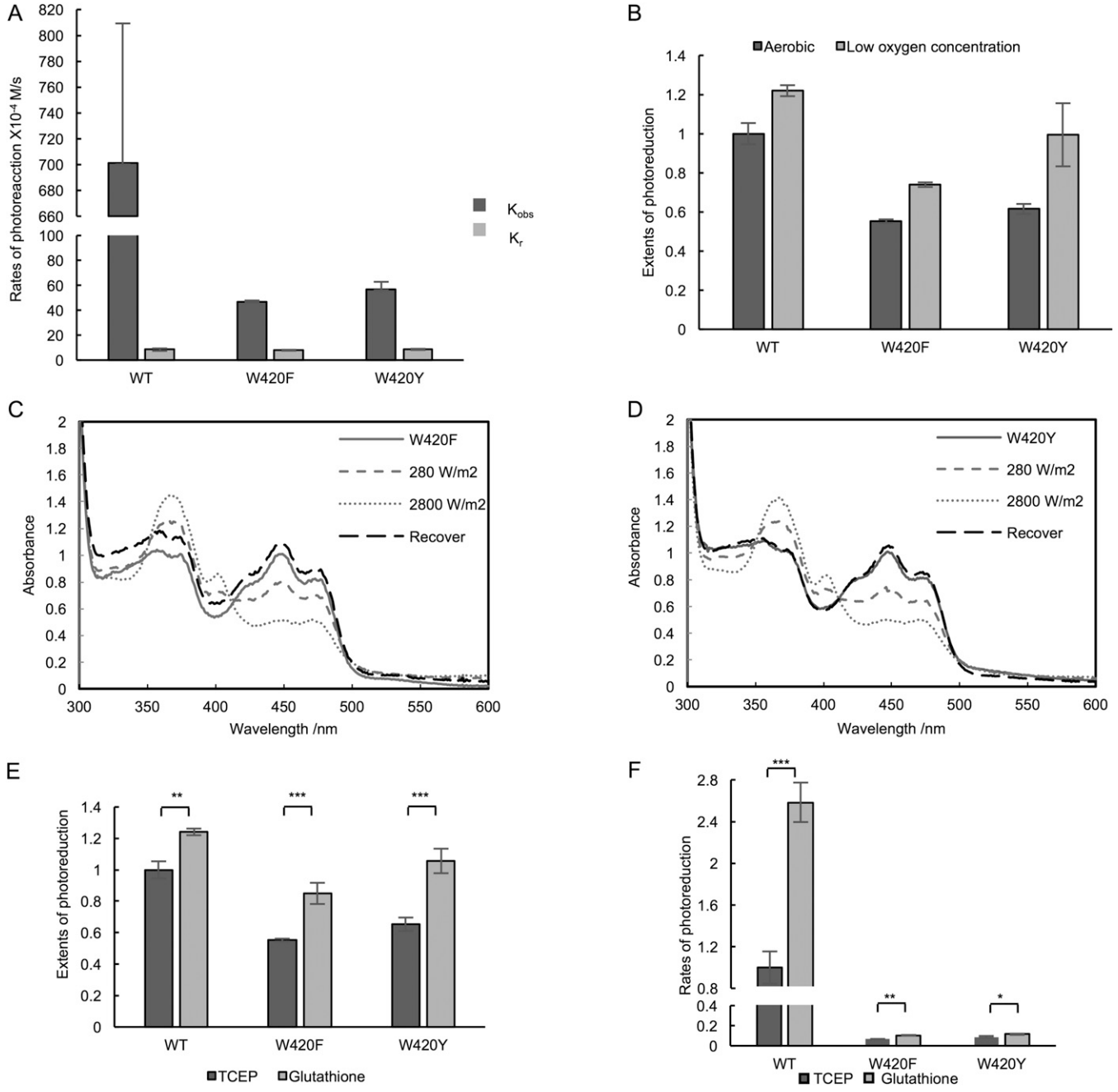

Fig. S1. Light intensity and reducing environment affect the extent of flavin photoreduction. (*A*) Rates of photoreduction at moderate light intensity (440 nm, 280 W/m^2, 15 min; black) vary among WT and 420 variants, while recovery rates in the dark (1 h; gray) are similar among the variants. (*B*) Low oxygen concentration maintained by the glucose oxidase-catalase enzyme system increases the extent of photoreduction (440 nm, 280 W/m^2) compared with aerobic photoreduction. Normalization as in Fig. 2*B*. Photoreduction and recovery are reversible, thereby indicating that the extent of incomplete reduction reflects this photochemical equilibrium and does not result from protein damage or oxidation during illumination. (*C* and *D*) W420F(Y) sample (solid line) is partially reduced in moderate light intensity (dashed line; 440 nm, 280 W/m^2, 15 min), which can be further reduced by high light intensity (dashed line; 440 nm, 2,800 W/m^2, 15 min). Following photoreduction, dCRY is oxidized after 1 h in the dark. (*E* and *F*) Photoreduction depends on the reducing agent. The extents (d) and rates (e) of photoreduction with either 2 mM TCEP (dark bars) or GSH (light bars) at moderate light intensity (440 nm, 280 W/m^2) after 15 min are shown. Normalization as in Fig. 2*B*. Error bars reflect the SEM for $n = 3$. *$P < 0.05$, **$P < 0.01$, ***$P < 0.005$; two-tailed, unpaired t test.

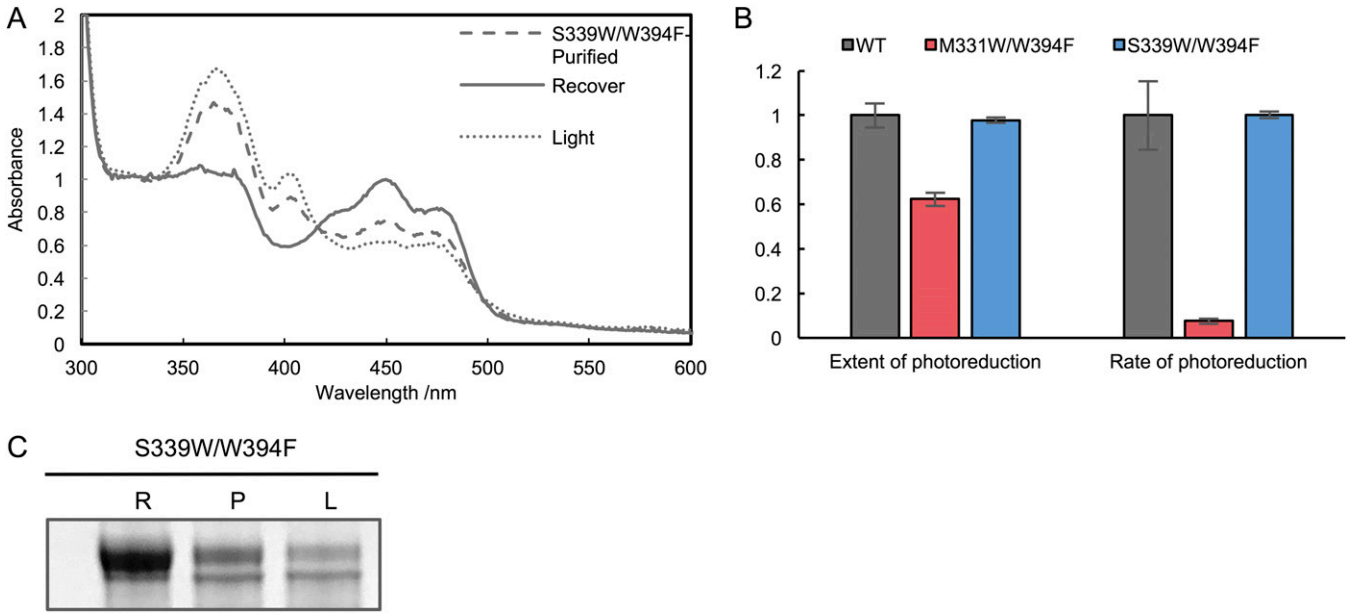

Fig. S2. Characterization of S339W/W394F. (*A*) Purified S339W/W394F contains mainly reduced flavin in ambient light as shown by UV–visible absorption spectroscopy. The surface variant is completely reduced under moderate light intensity (light, dashed line; 440 nm, 280 W/m^2, 15 min) and recovered to the oxidized state after 2 h (recover, dashed line). (*B*) Extent and rates of photoreduction at moderate light intensity (440 nm, 280 W/m^2, 15 min) of surface Trp variants. Normalization as in Fig. 2*B*. (*C*) CTT is partially released in the purified (P) S339W/W394F sample (as shown by trypsin digestion and SDS/PAGE) but recovers (R) protection after dark incubation and releases again after light exposure (L).

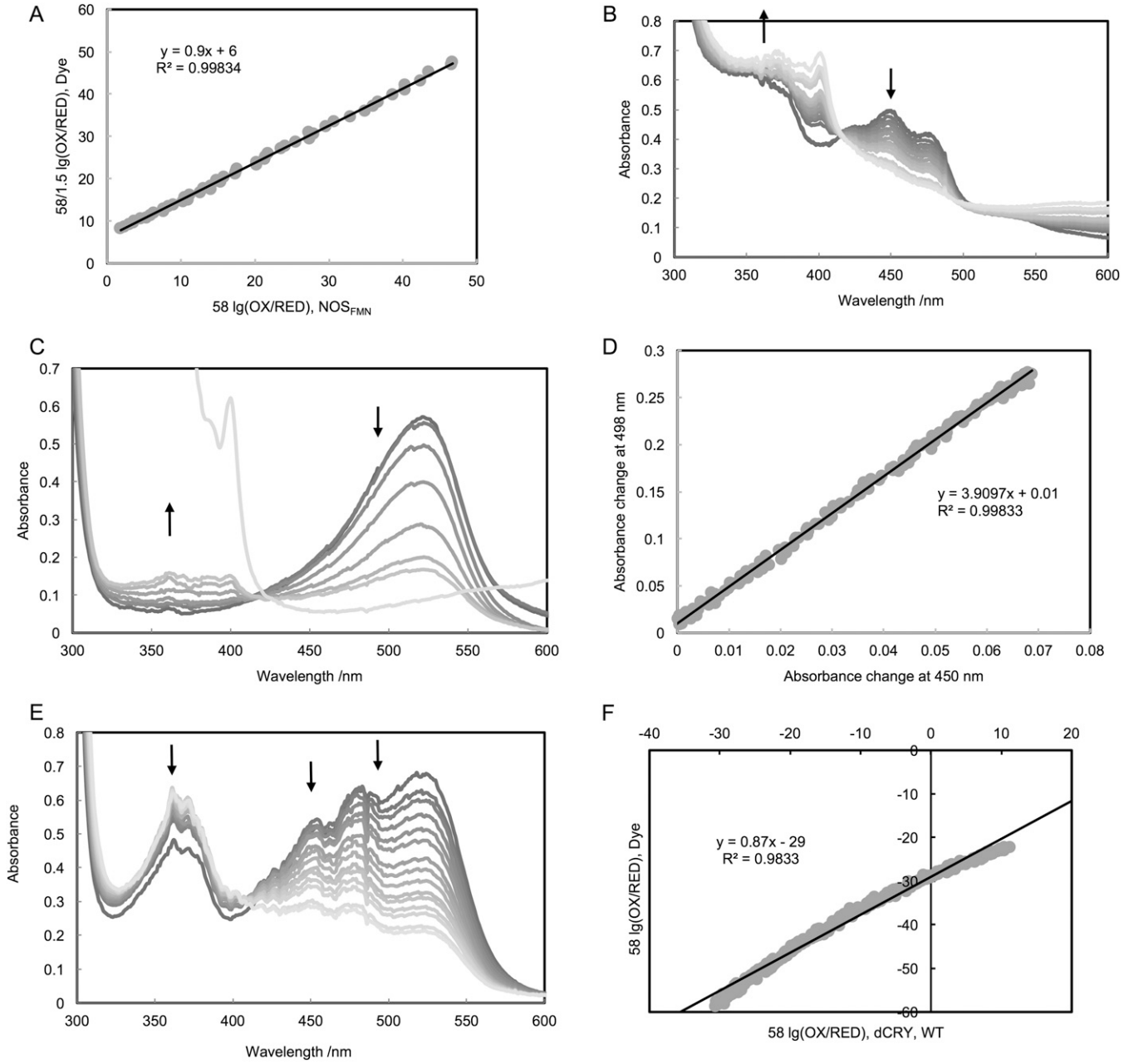

Fig. S3. Protein spectrum electrochemistry. (*A*) Nernst plot of Cresyl violet, ($E^{\circ\prime} = -177$ mV vs. SHE) vs. NOS_{FMN}. (*B*) dCRY WT anaerobic reduction by xanthine and xanthine oxidase as shown by an absorbance increase at 365 nm and decrease at 450 nm (arrows). An isosbestic point at 498 nm indicates the presence of FADox with $FAD^{\bullet-}$, but no further reduction to the hydroquinone. UV–visible (UV/Vis) spectra are shown for every 2 min over 1 h of reduction. (*C*) Safranin T anaerobic reduction by xanthine and xanthine oxidase gives an absorbance increase at 365 nm and decrease at 498 nm (arrows). UV/Vis Spectra are shown for every 2 min, while the last spectrum is taken after dithionite addition. (*D*) Relation between the absorbance change at 498 nm vs. 450 nm for safranin T. (*E*) WT dCRY is reduced by xanthine/xanthine oxidase in the presence of safranin T [$E^{0\prime} = -289$ mV (pH 7) vs. SHE] as indicated by an absorbance increase at 365 nm and decreases at 450 nm and 498 nm (arrows). A broad dye band appears at 522 nm. UV/Vis spectra are shown for every 2 min over 1 h of reduction. (*F*) Nernst plot of safranin T ($E^{0\prime} = -289$ mV vs. SHE) vs. dCRY WT.

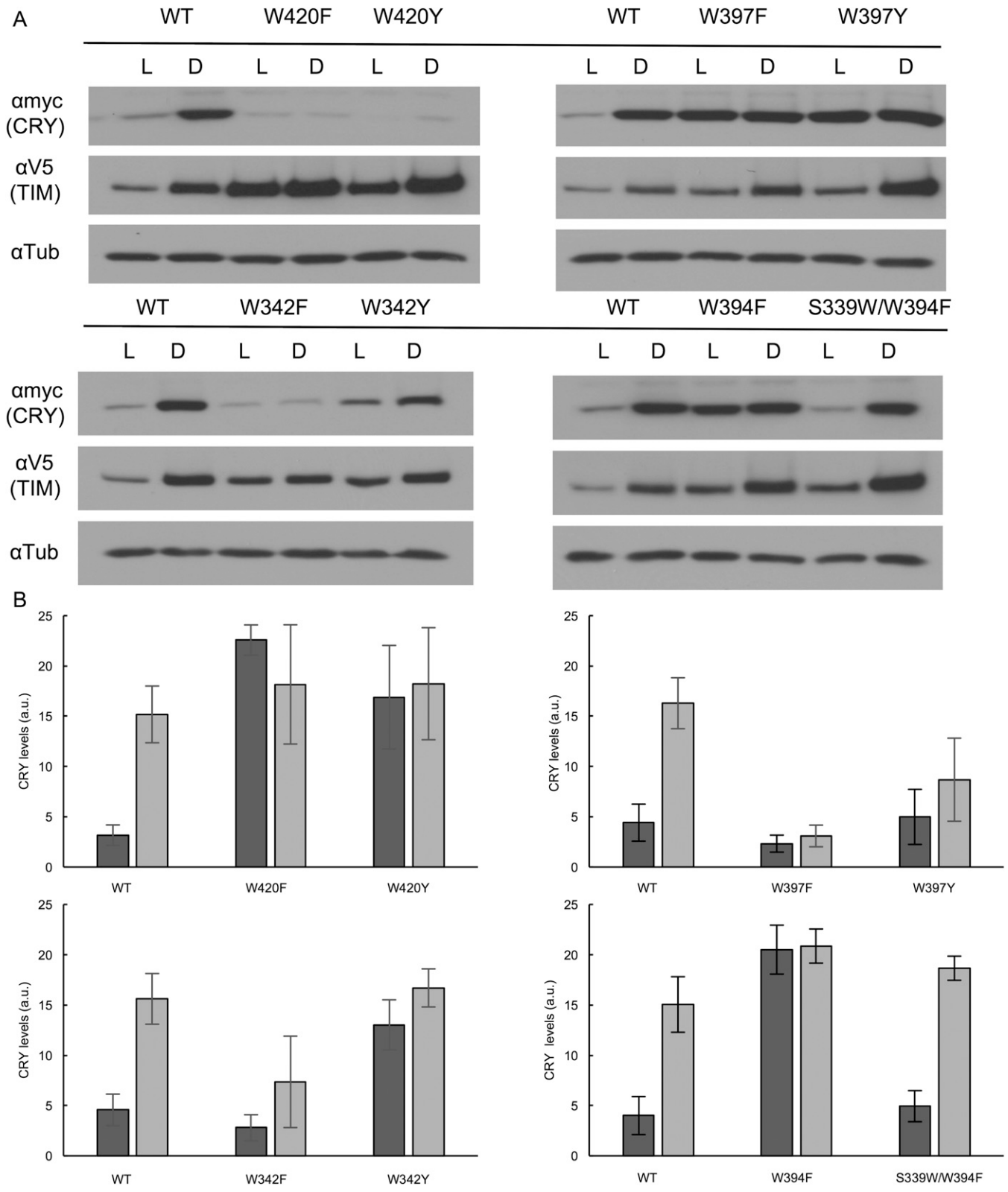

Fig. S4. CRY expression level in S2 insect cells. (*A*) Representative Western blots of epitope-tagged dCRY and TIM levels. D, dark sample; L, light-exposed sample (600 lx for 60 min). (*B*) Amount of dCRY in the dark (black column) and light (white column) relative to loading controls. Error bars reflect the SEM for $n = 4$.

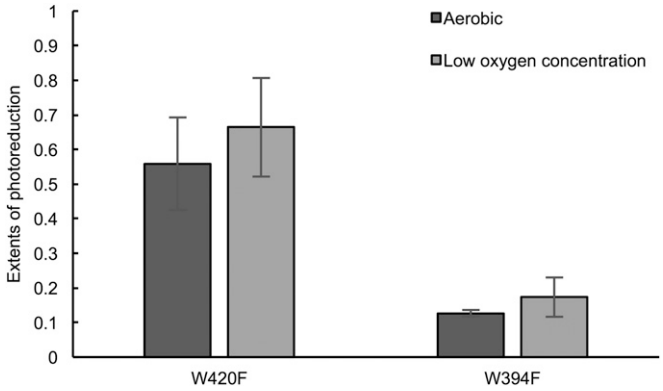

Fig. S5. Photoreduction of CRY variants. The extent of photoreduction with 2 mM GSH as a reductant at low light intensity, while low oxygen concentration (gray column) promotes the reduction compared with the aerobic condition (black column). Normalization as in Fig. 2*B*. Error bars reflect the SEM for $n = 3$.